J. Fluid Mech. (1997), *vol.* 334, *pp.* 189–210

Free-surface effects on spin-up in a rectangular tank

By J. A. VAN DE KONIJNENBERG AND G. J. F. VAN HEIJST

Fluid Dynamics Laboratory, Department of Technical Physics, Eindhoven University of Technology, PO Box 513, 5600 MB Eindhoven, The Netherlands

(Received 8 January 1996 and in revised form 5 August 1996)

The dependence of spin-up in a rectangular tank on deformation of the free surface is investigated experimentally. The results agree with earlier experimental and numerical data about the motion of vortices over topography. However, the presence of sidewalls appears to interact with the vortex drift induced by the surface topography. This combined effect provides a qualitative explanation for the observed behaviour of individual vortices. In particular, in the presence of free-surface deformation, cyclonic vortices in an elongated rectangle tend to drift away from the centre of the tank, so that their merging in the centre is discouraged.

1. Introduction

The spin-up of a homogeneous fluid in a container from one state of solid-body rotation to another is a fundamental problem in rotating fluid dynamics. Most previous studies on this subject concerned the flow in a tank with circular cross-section (Greenspan & Howard 1963; Wedemeyer 1964; Weidman 1976; van de Konijnenberg & van Heijst 1995). Such flows remain azimuthally symmetric and acquire a higher angular velocity through a weak secondary flow in the radial direction driven by Ekman layers at the bottom and, if present, at the lid of the container. By the vortex stretching coupled with this radial motion, the flow relative to the rotating tank can be proven to decay on a time scale $H/(\nu\Omega)^{1/2}$, with H the depth, ν the kinematic viscosity and Ω the final angular velocity (Greenspan & Howard 1963). Recently, the spin-up in containers with non-circular cross-sections has become the subject of investigation (van Heijst 1989; van Heijst, Davies & Davis 1990; van de Konijnenberg *et al.* 1994; Suh 1994). Spin-up flows in non-circular tanks are generally characterized by separation from the sidewall, a phenomenon caused by a pressure gradient along the sidewall of the initial flow field. This boundary-layer detachment provides an efficient mechanism for the transport of sidewall vorticity to the interior of the flow, leading to the formation of vortices and the break-up of the initial flow field. Despite possible three-dimensional instabilities at the beginning of the experiment, the flow is soon stabilized by its rotation, and becomes approximately two-dimensional. Owing to the self-organizing property of two-dimensional flows, the velocity field usually evolves into a pattern consisting of a small number of vortices rotating in either direction, with dimensions comparable to the width of the tank. During the spin-up process, a secondary flow induced by Ekman pumping persists, providing a damping mechanism for the two-dimensional vortex motion. In a typical laboratory experiment, the damping time scale of this Ekman pumping is larger than

the time scale on which the two-dimensional vortex motions take place. For the flow in early stages, therefore, properties such as boundary layer separation, vortex motion and self-organization can be understood qualitatively without taking Ekman pumping into account. For the flow in later stages, however, the Ekman suction becomes important, in particular for the relation between the vorticity ω and stream function ψ of the organized flow.

The spin-up in a rectangular tank was first studied by van Heijst *et al.* (1990), who found that shortly after the impulsive increase in angular velocity, cyclonic vortices were formed at the downstream ends of the longer sidewalls. In a geometry with aspect ratio 3:1, these vortices were seen to move towards the centre of the tank, merging into a single cyclonic vortex. Alongside this vortex, anticyclonic vortices appeared, resulting in a stable pattern of three counter-rotating vortices. Van Heijst *et al.* attributed the inward motion to the deformation of the free surface caused by the rotation of the fluid. This assertion seemed to be confirmed by later experiments. It was found both experimentally and numerically (van de Konijnenberg *et al.* 1994; Suh 1994) that at low angular velocities, merging does not occur. In such experiments, a similar pattern of three counter-rotating cells appears, but with an anticyclonic vortex in the centre. However, more recent experiments performed with very high angular velocities show that a second transition between merging and non-merging exists. In certain experiments, merging does no longer occur, an observation challenging the assertion by Van Heijst *et al.*

This paper presents results of a number of spin-up experiments from rest in two rectangular geometries. Emphasis is put on the influence of the final angular velocity Ω on the evolution of the flow field. The final angular velocity enters the spin-up problem through two independent parameters: the Reynolds number $Re = \Omega L^2/\nu$ on the one hand, and the Froude number $F = 4\Omega^2 L^2/gH$ on the other hand. The Froude number represents the free-surface effect, and is a measure of the ratio between the Rossby radius $(gH)^{1/2}/2\Omega$ and the size of the tank. The experiments indicate that the qualitative evolution of the flow field depends on both parameters: for low angular velocities the flow is mainly determined by the Reynolds number, whereas for high angular velocities the flow also depends on the Froude number. In the context of rotating flows, often the Ekman number is used instead of the Reynolds number, in particular if emphasis is put on the spin-up time scale $H/(\nu\Omega)^{1/2} = E^{-1/2}\Omega^{-1}$. However, in spin-up in rectangular tanks the finite depth of the fluid is noticeable only at late times, when flow separation and vortex formation and possibly vortex merger have already taken place. For this reason we prefer to use the Reynolds number in this paper.

In §2, the experimental set-up is described. In §3, an analytical expression for the stream function of the starting flow is derived, in excellent agreement with experimental results. In §4, spin-up in a square tank is studied. For this geometry the flow appears to be dominated by an anticyclonic vortex in the centre of the tank. In §5, the aspect ratio of 9:4 is studied in more detail. This section contains a sequence of four experiments differing only in the final angular velocity Ω. In §6, the qualitative influence of bottom topography on the two-dimensional vortex motion during spin-up process is investigated experimentally. Since the bottom topography is analogous with the deformation of the free surface, these experiments can be used to distinguish the influence of the Reynolds number and free-surface deformation in experiments with high angular velocity.

2. Experimental set-up

The spin-up experiments were performed by using a tank filled with tap water, placed centrally on a rotating table. At $t = 0$, the angular velocity of the table was suddenly changed from $\Omega - \Delta\Omega$ to Ω, and was thereafter kept at this value during the experiment. It was verified that fluctuations in the final angular velocity are very small compared with the final angular velocity used in the experiments. Two tanks were used: a square tank with sides $2L = 80$ cm, filled to a depth of 20 cm, and a rectangular tank with length $2L = 88.6$ cm and width $2B = 38.9$ cm, filled to a depth of 35 cm. The latter geometry was chosen because of its tendency to lead to an array of three vortex cells that may have either orientation, depending on whether or not vortex merger occurs early in the experiment. This makes this aspect ratio convenient to demonstrate the influence of the final angular velocity on the spin-up flow. In the square tank the angular velocity was increased from 0 to 0.24 rad s^{-1} and from 0 to 1.0 rad s^{-1}, corresponding to a Rossby radius of 2.9 and 0.70 m, respectively. In the rectangular tank the angular velocity was increased from rest to 0.035, 0.24, 1.0 and 1.7 rad s^{-1}, corresponding to a Rossby radius of 26, 2.1, 0.93 and 0.54 m, respectively.

Quantitative results were obtained with small tracer particles floating on the surface of the fluid. Dye was added to the water in order to increase the contrast between the fluid and the particles. First, a video recording of the flow was made with a video camera corotating with the tank. Then, after the experiment, the recording was processed by a PC equipped with a frame grabber. For this purpose an adapted version of the DigImage system developed by Dalziel (1992) was used. This is an image processing system that allows the tracking of particles in a cycle of three stages: (i) a sequence of 16 video images is captured and stored in the memory of the frame grabber; (ii) in each image, particles are located, this procedure being based on a number of user-defined criteria such as brightness and size; (iii) particles in subsequent images corresponding to the same physical particle are identified. In this procedure, matchings at earlier times are used to estimate the positions of the particles in the next video frame. After the particle paths have been obtained, the positions are stored, and the cycle is repeated. Further processing of these data was done by an extension to the DigImage software developed by van der Plas (1994). This option provides the possibility to extract data files containing the particle velocities from the data file created by the particle tracking routine. The vorticity was obtained by matching the data with spline functions and manipulating the coefficients of this expansion. The stream function was calculated from the vorticity by using a Poisson solver. In this way the stream function of the solenoidal component of the velocity field is calculated, which is more elegant than applying integration techniques if the flow is not exactly divergence free. According to the amount of scatter in graphs of the vorticity versus the stream function if the flow is almost steady (see e.g. figure 3 at $t = 960$ s), the errors in the experimental data are of the order of a few percent. For more detailed information about the data-processing method, see Nguyen Duc & Sommeria (1988).

In addition to those with particles, experiments were performed with a small amount of dye added to the otherwise clear tap water. In this way, a qualitative impression of the flow field could be obtained. Except for the case of spin-up from rest to 0.035 rad s^{-1}, the flow was seen to be turbulent shortly after the increase in angular velocity of the tank; however, the flow always relaminarized early in the experiment, and remained approximately two-dimensional afterwards.

The experimental flow field can be disturbed by several effects. Small quantities of surface-active matter can lead to an irregular, asymmetric motion at the surface, especially at low angular velocities. This problem was overcome by adding a small amount of wetting agent to the water. This causes a reduction of the surface tension, making the observed flow more symmetric and smooth.

Temperature differences in the water in the tank, possibly caused by evaporative cooling at the free surface, the heat produced by the drive mechanism of the table or temperature differences between the water and the laboratory air, can drive weak convective flows (see e.g. Boubnov & Golitsyn 1986; Boubnov & van Heijst 1994). In many experiments, it was observed that at later times the flow field becomes irregular, with a tendency for small, axially aligned vortices to appear. This effect was reduced by allowing the water to assume room temperature over a period of at least 12 hours, and by using a (transparent) rigid lid on top of the tank, which was typically 10 cm above the level of the free surface. Such a lid was used in all experiments with a spin-up time scale larger than five minutes.

3. Starting flow

The flow immediately after the impulsive increase in angular velocity is characterized by a uniform vorticity -2Ω in a system corotating with the tank. Since the vorticity is related to the stream function by

$$\omega = -\nabla^2\psi, \tag{3.1}$$

this leads to a Poisson equation for the stream function ψ of the flow relative to the rotating tank:

$$\nabla^2\psi = 2\Omega. \tag{3.2}$$

Because of the zero-normal-flow condition, the sidewall boundary coincides with a streamline, the stream function of which is taken to be zero. The problem for ψ is solved by first finding a convenient particular solution ψ_{part} that takes away the inhomogeneous right-hand side of (3.2), and subsequently solving the remaining Laplace equation for $\psi - \psi_{part}$, with inhomogeneous boundary conditions to compensate for the non-zero values of ψ_{part} at the sidewalls. The resulting solution can be written as

$$\psi(x,y) = \Omega(x^2-L^2) + \frac{4\Omega L^2}{\pi^3}\sum_{n=0}^{\infty}\frac{(-1)^n}{(n+\frac{1}{2})^3}\cos(n+\tfrac{1}{2})\pi x/L\,\frac{\cosh(n+\frac{1}{2})\pi y/L}{\cosh(n+\frac{1}{2})\pi B/L}. \tag{3.3}$$

This expression is also valid for $B > L$, and could have been written equally well with x exchanged with y and, simultaneously, B exchanged with L; the only difference would be a slightly different convergence speed for a given aspect ratio L/B. A similar expression was derived earlier by van Heijst *et al.* (1990); our version is somewhat simpler because of the more convenient choice of coordinate system. In turn, the solution by van Heijst *et al.* appeared later to be a rediscovery of a solution by Stokes (1843) for the flow in a moving rectangle in a non-rotating coordinate system.

A numerical evaluation of (3.3) up to 10 terms is compared with experimental data in figures 1 and 2. Although the experimental data are slightly asymmetric with respect to the centre of the tank, the analytical and experimental results are in good agreement.

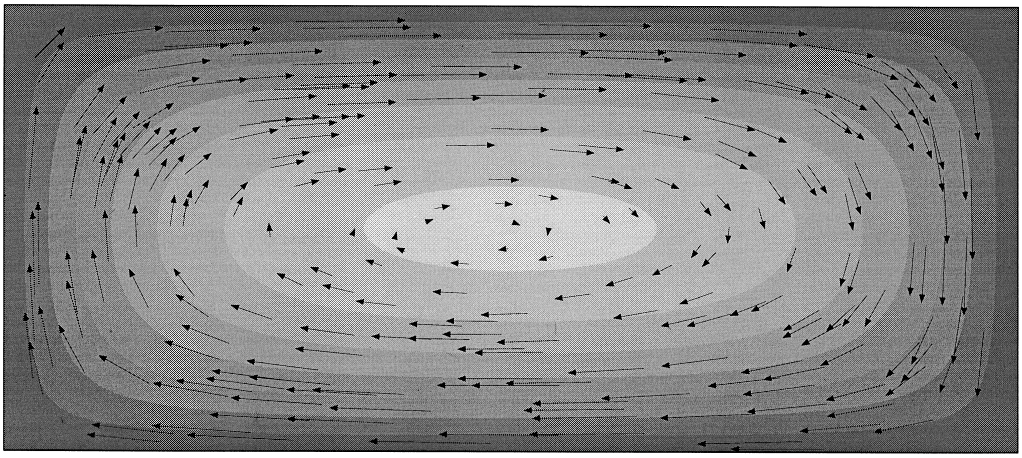

FIGURE 1. Starting flow in a rectangular tank with length 88.6 cm and width 38.9 cm according to (3.3) and to an experiment in which the angular velocity was increased from 0 to 0.035 rad s^{-1}. The analytically determined stream function is represented by the graded shading. The arrows correspond to particles floating on the free surface as they were tracked by the DigImage system.

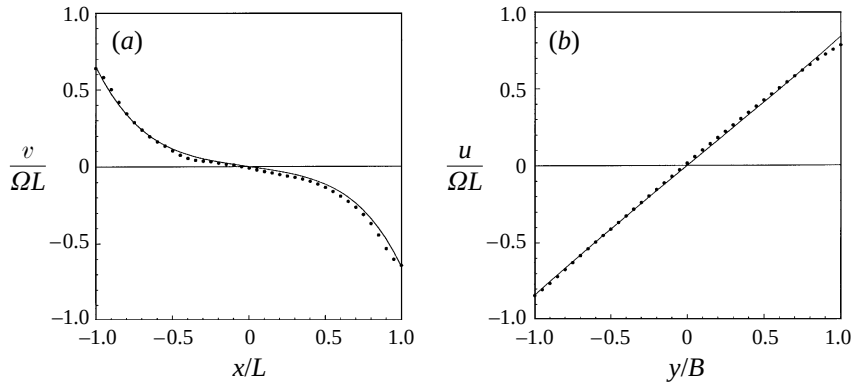

FIGURE 2. Velocity profiles at $y = 0$ (a) and $x = 0$ (b) of the starting flow in a rectangular tank with length 88.6 cm and width 38.9 cm according to (3.3) and to measurements at the free surface. The solid curves correspond to the analytical solution, the filled circles to the experimental results.

4. Spin-up in a square tank

The experiments discussed in this section were performed in a tank with sidewalls with length $2L = 80$ cm and a fluid depth of 20 cm. Experimental results of spin-up from rest to 0.24 and to 1.0 rad s^{-1} are presented in figures 3 and 4. The graphs for $t = 0$ correspond to the starting flow. Close to the boundaries (ψ close to zero) the data of the vorticity deviate from the theoretical uniform profile. This difference is caused by the finite distance from the sidewall to the nearest particles: the experimental method does not resolve structures smaller than the distance between the particles or from the sidewall to the particles. In all experiments, the zero-velocity condition is imposed by adding zero vectors along the boundary. In the algorithm for computation of the vorticity, a shear layer with thickness equal to the distance from the sidewall to the nearest particles is assumed. Since the velocity close to the sidewall is higher than in the centre, this boundary layer corresponds to a rather broad stream

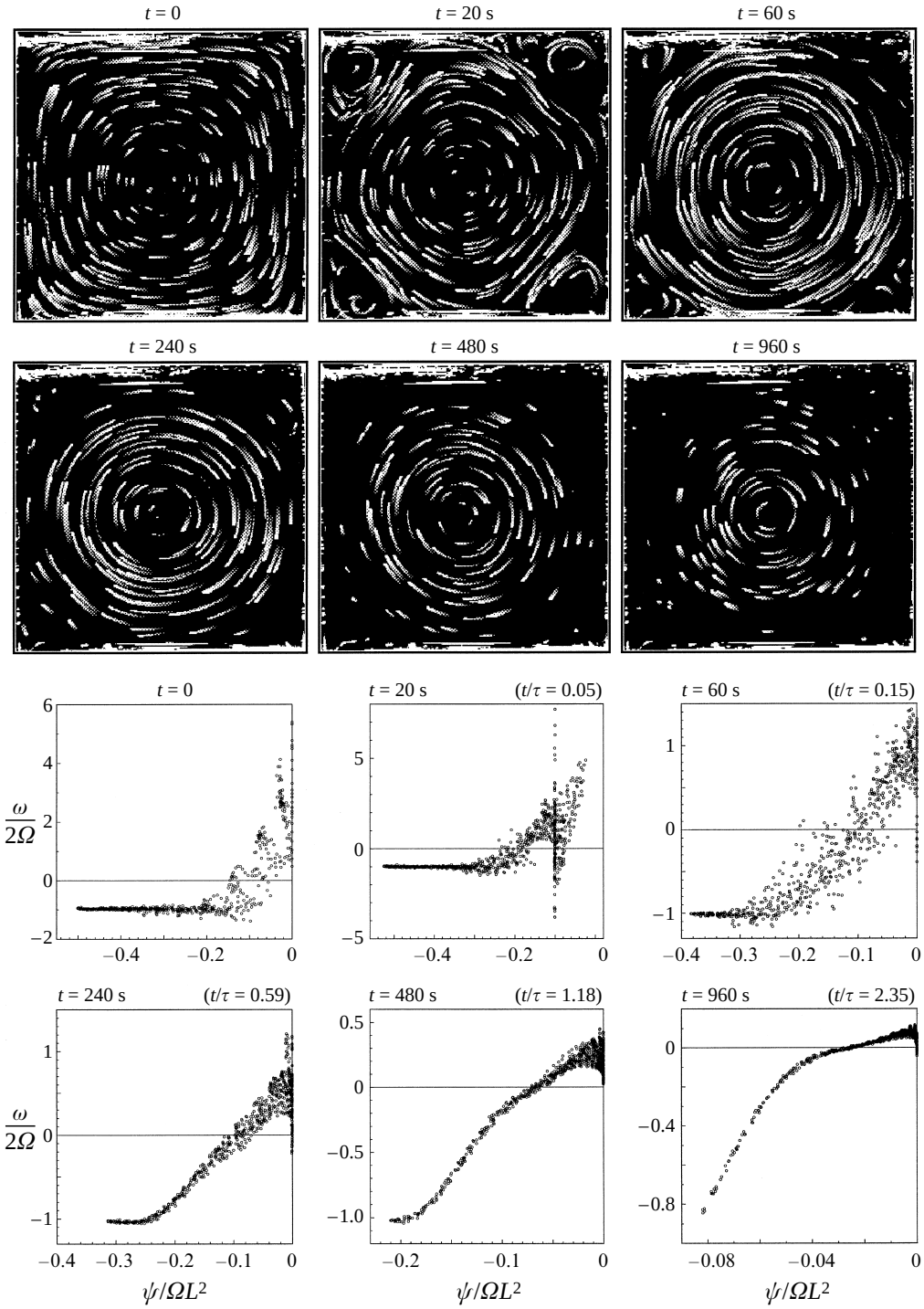

FIGURE 3. Particle paths and $\omega(\psi)$-scatterplots for spin-up from 0 to 0.24 rad s^{-1} in a square tank with sides $2L = 80$ cm and depth $H = 20$ cm. The lengths of the particle paths for the different pictures are not representative of the speeds of the particles, but were chosen to yield a good impression of the velocity field. The time has been non-dimensionalized with $\tau = H/(\nu\Omega)^{1/2}$.

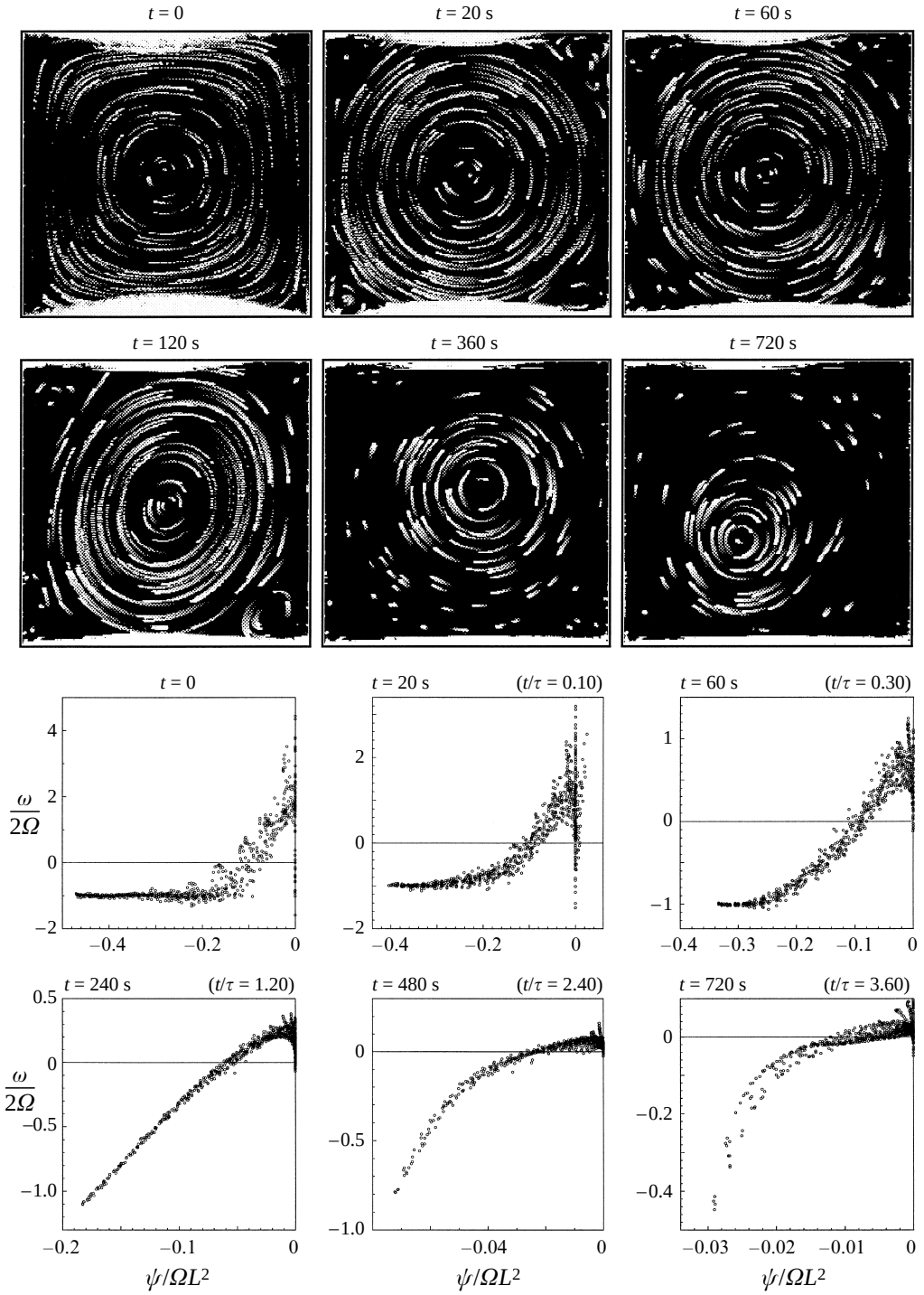

FIGURE 4. As in figure 3, but now for spin-up from 0 to 1.0 rad s^{-1}.

function interval. The shear layer is only present at $t = 0$; at later times the limited spatial resolution is of less importance.

The starting flow quickly loses its initial appearance: the separated flow is unstable, and dye visualizations indicate that even in the $0 \rightarrow 0.24$ rad s^{-1} experiment, the cyclonic vortices are three-dimensionally turbulent. Because of this turbulence, and the fact that in a square tank they are relatively weak, the corner vortices disappear quickly. The time scale on which the turbulence disappears is of the order of several minutes. By this time the flow is dominated by an approximately circular anticyclonic core vortex. The core behaves in much the same way as in the case of spin-up in a circular tank discussed by van de Konijnenberg & van Heijst (1995). Initially, a large part of the domain has relative vorticity -2Ω, but due to the inward secondary motion caused by the Ekman-pumping mechanism, this region decreases slowly in size.

The curvature of the $\omega(\psi)$-graph changes in the course of the experiment, an effect caused by the nonlinearity of the Ekman suction term in the equation for the relative vorticity. Consider the two-dimensional vorticity equation in a system rotating with angular velocity Ω, given by

$$\frac{\partial \omega}{\partial t} + \boldsymbol{u} \cdot \nabla \omega = -(\omega + 2\Omega)\nabla \cdot \boldsymbol{u} + \nu \nabla^2 \omega; \tag{4.1}$$

where $\boldsymbol{u}$ denotes the relative velocity in the horizontal plane, and ω is the relative vorticity. Although the three-dimensional flow is assumed to be strictly incompressible, the vorticity equation is given here in its compressible form. The reason is that $\nabla \cdot \boldsymbol{u}$ is slightly non-zero because of the Ekman pumping; the term containing $\nabla \cdot \boldsymbol{u}$ represents the vortex stretching/squeezing due to the small vertical velocity at the top of the Ekman layer. It was shown by Greenspan & Howard (1963) that this Ekman pumping velocity is a linear function of the relative vorticity if the flow is linear, that is, if the relative velocities are very small. Numerical calculations by Rogers & Lance (1960) suggest that this linear dependence is a reasonable approximation for moderately nonlinear flows as well, a property used by Wedemeyer (1964) to obtain an analytical expression for the velocity field of nonlinear spin-up in a circular container. Since the Ekman pumping velocity is proportional to the two-dimensional divergence, (4.1) is approximately quadratic in ω. This implies that high relative vorticities will decay rapidly, whereas for $\omega = -2\Omega$, Ekman suction is ineffective, and the vorticity can increase through viscous diffusion only.

During the first stages of the experiment, the vorticity in the centre of the tank is still equal to -2Ω, unaffected by Ekman pumping. In contrast, the positive vorticity in the outer regions decreases rapidly. As a result, the appearance of the $\omega(\psi)$-graphs changes in the course of the experiment, becoming flatter in the positive-vorticity part, and steeper in the negative-vorticity part. This interpretation agrees with a general property of the $\omega(\psi)$-graph of its slope being inversely proportional to the area of the vortex structure it represents†.

† Consider a circular vortex with radius a and a linear relation between vorticity and stream function, so that $\omega = k^2\psi$. In that case one finds that $\psi(r) = AJ_0(kr)$ and $\omega(r) = Ak^2J_0(kr)$. Imposing $\partial\psi/\partial r = 0$ at $r = a$ leads to $k = j_{1n}/a$, with j_{1n} the nth zero of J_1. Such vortices are known as Bessel vortices. The solution with $n = 1$ ($k = 3.8317/a$) has a unidirectional flow and is often used as a convenient vortex model in analytical and numerical investigations. For all Bessel vortices, the slope k^2 of the $\omega(\psi)$-graph is inversely proportional to a^2. Since the stream function is defined up to an arbitrary constant, this argument can be applied to any linearly ending branch in a $\omega(\psi)$-graph.

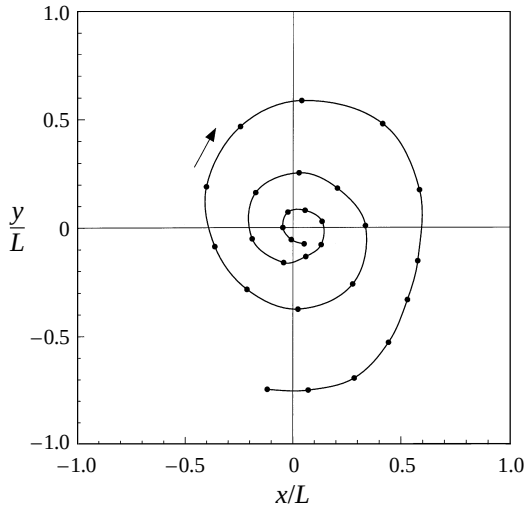

FIGURE 5. Trajectory of the centre of the anticyclonic vortex in the square tank for a spin-up experiment from 0 to 1.0 rad s^{-1}. The dots represent the position of the vortex centre after 30 s intervals, starting from $t = 240$ s at the centre of the tank and ending at $t = 1080$ s near one of the sidewalls.

For high angular velocities there is an outward motion of the central anticyclonic vortex, as shown by the particle paths at 720 s in figure 4. This effect is probably caused by the depth gradient caused by the deformation of the free surface. According to earlier research (McWilliams & Flierl 1979; Carnevale, Kloosterziel & van Heijst 1990), both cyclonic and anticyclonic vortices show a horizontal drift in the presence of bottom or surface topography. Most of the investigations of rotating flows over topography were inspired by applications in a geophysical context. The terminology used in these papers is still reminiscent of this geophysical background. Using the analogy between rotating flows over topography and geophysical flows involving a latitude dependence of the Coriolis parameter, the shallow part of the tank is commonly referred to as the 'north' and the deeper part as the 'south'. Experimental and numerical investigations have revealed that small cyclonic vortices on large-scale topography show a drift towards the northwest, and anticyclonic vortices towards the southwest. In the square tank, the centre is the shallower part and corresponds to the north, the outer regions near the sidewalls and in the corners are the deeper parts and correspond to the south. This means that small cyclonic vortices tend to move towards the centre, whereas small anticyclonic vortices tend to move away from it.

Although in this case the anticyclonic vortex is comparable in size with the length scale of topography variations, the assumption that its motion is determined by the rules found for smaller vortices may lead to a qualitative understanding of the observed drift in figure 4. In order to make a qualitative comparison between this drift and the previously mentioned results of earlier research, measurements of the position of the centre of the core were performed for a spin-up experiment from 0 to 1.0 rad s^{-1}; the results are given in figure 5. The data were obtained by manually tracking the position of a small particle floating on the surface of the fluid close to the centre of the core. Owing to the slightly off-centred position of the particle and the rotation of the core, the particle followed a cycloidal motion instead of the smooth curve represented in figure 5. Since the excursions caused by the fast

revolutions around the core centre were much smaller than the distance between the spiral arms, the position of the centre could be estimated accurately. Dye was added in the beginning of the experiment to investigate the deformation of the core due to interaction with the sidewalls. Deformation of the core due to secondary vorticity at the sidewalls was seen to become important after approximately 18 minutes; by that time the core has become very weak due to the Ekman-pumping mechanism.

According to figure 5, the core moves outward in a clockwise spiroid motion to the local southwest. This agrees qualitatively with the results of Carnevale *et al.* (1991). Experiments were conducted using bottom topography with the deeper part in the centre to confirm that the instability of the central position of the core is induced by topography. According to the 'southwest' rule for anticyclonic vortices, this implies that the position of the core in the centre of the tank is stabilized, and indeed no outward motion was observed in these experiments. Owing to the motion of the anticyclonic vortex, the flow in the $0 \rightarrow 1.0$ rad s^{-1} experiment loses part of its quasi-steady nature, as can be seen from the scatter in the $\omega(\psi)$-graph at 720 s (figure 4). It has been verified that the scatter in the left-hand side of the graph disappears in a coordinate system that moves with the anticyclonic vortex.

Though present for any angular velocity, in the geometry described in this section, the instability of the core is significant for angular velocities larger than 1 rad s^{-1} only. For a fluid depth of 20 cm this corresponds to a maximum surface elevation of only a few percent. At a higher angular velocity, the deformation of the surface is stronger, and the outward motion is faster. In that case, the core has more energy left when it reaches the sidewall, and its radial velocity is higher. The core then induces positive vorticity at the sidewall, forming a small cyclonic vortex that combines with the core to form an asymmetric dipole. This structure travels in a circular path through the tank until it hits the sidewall once again. During this process the core dissipates its energy by Ekman pumping, filamentation and friction caused by the two-dimensional motion, until finally all motion has decayed and the spin-up process is complete.

5. Spin-up in a tank with aspect ratio 9:4

5.1. *Spin-up from 0 to 0.035 rad s^{-1}*

The experimental results for the starting flow and the further evolution of the flow field are presented in figure 6. Soon after the start of the experiment, cyclonic vortices are formed in each corner of the flow domain. The vortices in the downstream corners of the shorter sidewalls are weak, and disappear quickly. Owing to the high velocities at the longer sidewall and the correspondingly stronger advection towards the downstream corners, the vortices in the downstream corners of the longer sidewalls become much stronger, and grow in size until they obtain a diameter comparable to the width of the tank. This results in a three-cell configuration, which appears to be stable: the vortices do not drift away or change in size or shape, but decay slowly from the combined effect of the Ekman-pumping mechanism and viscous decay in the horizontal plane.

The flow pattern consisting of these two cyclonic vortices, together with the central anticyclonic vortex, resembles a tripolar vortex, such as described by van Heijst & Kloosterziel (1989) and van Heijst, Kloosterziel & Williams (1991). This vortical structure tends to rotate until the walls of the tank inhibit further motion. However, the tripolar vortex discussed by van Heijst *et al.* (1991) moves around in an infinite domain, whereas in this case, the presence of sidewalls makes the situation more

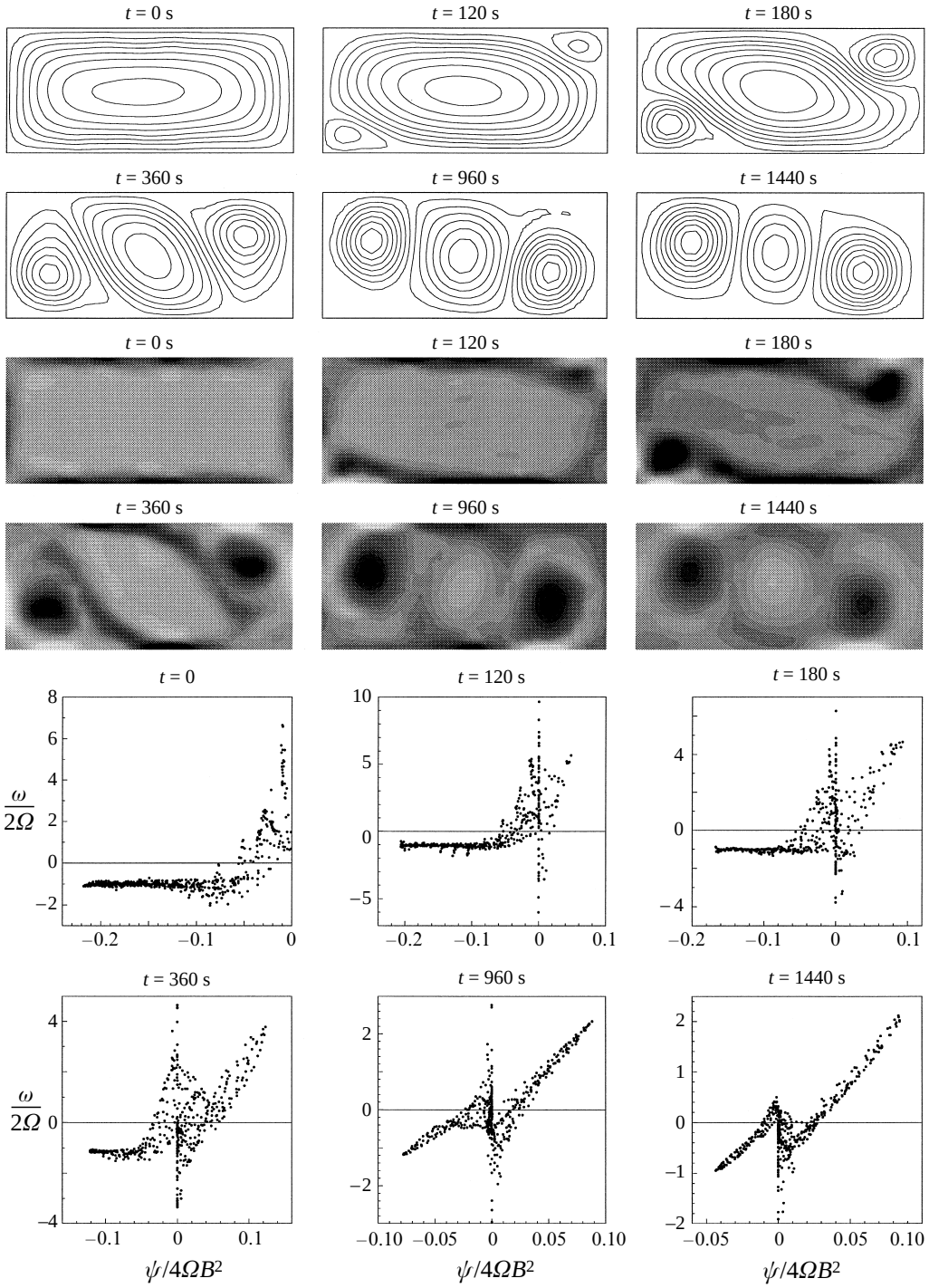

FIGURE 6. Experimental results for spin-up from 0 → 0.035 rad s^{-1} in a rectangular tank with length 0.886 m, width 0.389 m and depth 0.35 m. Top plots show stream function, middle plots vorticity and lower plots $\omega(\psi)$.

complex. Additional experiments indicate that the tendency to rotate depends on the aspect ratio of the tank. In similar experiments in a tank of 120×40 cm, hardly any rotation was observed, and the cyclonic vortices remain close to the symmetry-axis.

The scatterplots in figure 6 provide information about the flow field that cannot be easily derived from the contour graphs. At $t = 0$, the flow has a uniform vorticity, leading to the single horizontal branch at $\omega/2\Omega = -1$. At $t = 120$ s, 180 s and 360 s at the left-hand side of the graphs this horizontal branch is still present, but the graphs take on a different appearance during the further evolution of the flow. In particular, points with $\psi > 0$ appear, corresponding to the formation of cyclonic vortices. At early times there is a significant amount of scatter, but a well-defined branch eventually emerges. The right-hand end of this branch corresponds to the centres of the cyclonic vortices; the place where it sprouts from the vertical branch at $\psi = 0$ corresponds to the outer parts of the cyclonic vortices. The collapse to a single branch implies that these vortices become increasingly stationary in the course of the experiment. The points at $\psi = 0$ with strongly positive or negative vorticity correspond to points close to the sidewall, at the edges of strong vortices; from the vorticity graphs in figure 6 it can be seen that each of the three dominating vortices induces oppositely signed vorticity at the sidewalls. The branch at the left-hand side of the scatterplots corresponds to the central anticyclonic cell. This vortex rapidly loses its uniform vorticity profile, an effect that can be ascribed to viscous diffusion, perhaps in combination with Ekman suction. Characteristic of the scatterplots is that the two dominating branches are staggered; each branch consists of a positive and a negative vorticity part. This behaviour can also be seen from the fact that each vortex in figure 6 is surrounded by oppositely signed vorticity. The staggering between the branches indicates that this oppositely signed vorticity is not only present close to the sidewalls, but also between the cells: each vortex is essentially an isolated structure.

The approximately linear appearance of the $\omega(\psi)$-graph at 1440 s in figure 6 makes it possible to check the relation between $\partial\omega/\partial\psi$ and the size of each vortex. Since a Bessel vortex with radius a has $\partial\omega/\partial\psi = j_{11}^2/a^2 = 14.7/a^2$ (see footnote in §4), we would expect $\partial\omega/\partial\psi$ to be close to $14.7/B^2$. An actual measurement leads to $\partial\omega/\partial\psi = 14/a^2$ for the anticyclonic vortex and $\partial\omega/\partial\psi = 17/a^2$ for the cyclonic vortex. In view of the cyclonic vortex being somewhat smaller than the anticyclonic vortex, these results are quite plausible.

Unfortunately, the very low angular velocity makes it difficult to shield the flow from external effects such as heating of the fluid by the drive mechanism of the rotating table, the laboratory air or the lighting used to illuminate the particles. As a result, the vorticity and stream function at $t = 960$ s and $t = 1440$ s are less accurate than other results presented in this paper. A comparison with numerical results (van de Konijnenberg *et al.* 1994) indicates that at these times, the measured cyclonic vortices are stronger than is to be expected in the absence of external effects. In previous experiments, the flow pattern sometimes had not decayed noticeably after several hours, indicating that some driving effect is present that is able to overcome the damping caused by viscosity and Ekman suction. The experiment in this section was performed in a tank placed inside a bigger tank that was also filled with water. The extra layer of water acts as a buffer for external heating and cooling, and the quality of the results (estimated from the symmetry of the flow field and the amount of scatter in the $\omega(\psi)$-plots) was seen to improve. Nevertheless, in all experiments at such low angular velocities the accuracy of the results was seen to deteriorate after 20 or 30 minutes.

5.2. *Spin-up from 0 to 0.24 rad s^{-1}*

The outcome of the experiment changes drastically if a final angular velocity of 0.24 rad s^{-1} instead of 0.035 rad s^{-1} is taken, as shown in figure 7. The consequences of a higher Reynolds number become manifest soon after the start of the experiment. Large cyclonic vortices are formed in a similar way as in the experiment from 0 to 0.035 rad s^{-1}, but also smaller structures appear: the smooth strips of positive vorticity from the sidewall to the core are seen to break up into smaller vortices merging into the main corner vortex later on.

A more striking effect, however, is the merging of the cyclonic vortices into one strong vortex in the centre of the tank. This phenomenon is observed only if the vortices approach each other closely enough, a condition well satisfied for this geometry; for this Reynolds number, the critical aspect ratio beyond which merging of the corner vortices no longer occurs appears to be about 4:1. Compared to the spin-up time scale, vortex merging is a rapid process. According to the streamline patterns, the merging takes place between 100 and 110 s. However, the vorticity graphs indicate that the merging is not quite completed at $t = 120$ s: the remnants of the original vortices can still be distinguished in the core of the newly formed vortex. As these parts wrap around each other more closely, the amount of scatter in the $\omega(\psi)$-graphs decreases, until a well-defined relationship remains; this can be seen in the scatterplot at $t = 240$ s. A similar merging of the cyclonic corner cells was observed earlier by van Heijst *et al.* (1990) in a tank with an aspect ratio of 3:1.

Although it is not clear whether a simple argument can be given why merging takes place in this experiment, and not in the experiment from 0 to 0.035 rad s^{-1}, it seems likely that this difference is coupled with the Reynolds number. In the $0 \rightarrow 0.035$ rad s^{-1} experiment the cyclonic vortices may be damped too strongly to develop the high velocity gradients coupled with the merging process, or the vorticity of the corner vortices in the $0 \rightarrow 0.24$ rad s^{-1} experiment may be more concentrated, making them smaller and more mobile. Van Heijst *et al.* (1990) attributed the inward motion of the cyclonic vortices to an imbalance between centrifugal and Coriolis forces caused by free-surface deformation and the topography-induced drift according to the rules found for small vortices discussed in §4. However, in subsequent sections it is shown that free-surface deformation in combination with the presence of the sidewalls gives rise to the opposite behaviour.

At late times the central cyclonic vortex is affected by the interaction with its surroundings, and loses some of its stationarity. The graphs at $t = 480$ s show that the vortex becomes elliptical; the axes of the ellipse slowly rotate in a cyclonic direction. Dye visualizations indicate that the non-stationarity of the cyclonic vortex involves filamentation and mixing of the outer layers with the surroundings. This interaction process affects the $\omega(\psi)$-scatterplot as well. The shape of the branch corresponding to the centre of the cyclonic vortex at $t = 480$ s can still be recognized from the previous scatterplot, but the part corresponding with the outer region of the cyclonic vortex ($0 < \psi/4\Omega B^2 < 0.04$) is affected in its shape and in the amount of scatter. The anticyclonic vortices alongside the central cyclonic cell are less stable than in the $0 \rightarrow 0.035$ rad s^{-1} experiment and keep changing in size and shape. Nevertheless, they show the same preference for a position off the horizontal axis, but since the central cell is now cyclonic, the flanking cells are now shifted in a cyclonic sense.

Both the scatterplots at $t = 60$ s (before the merging) and at $t = 240$ s (after the merging) show an upward-curving relationship between ω and ψ. This reminds one of

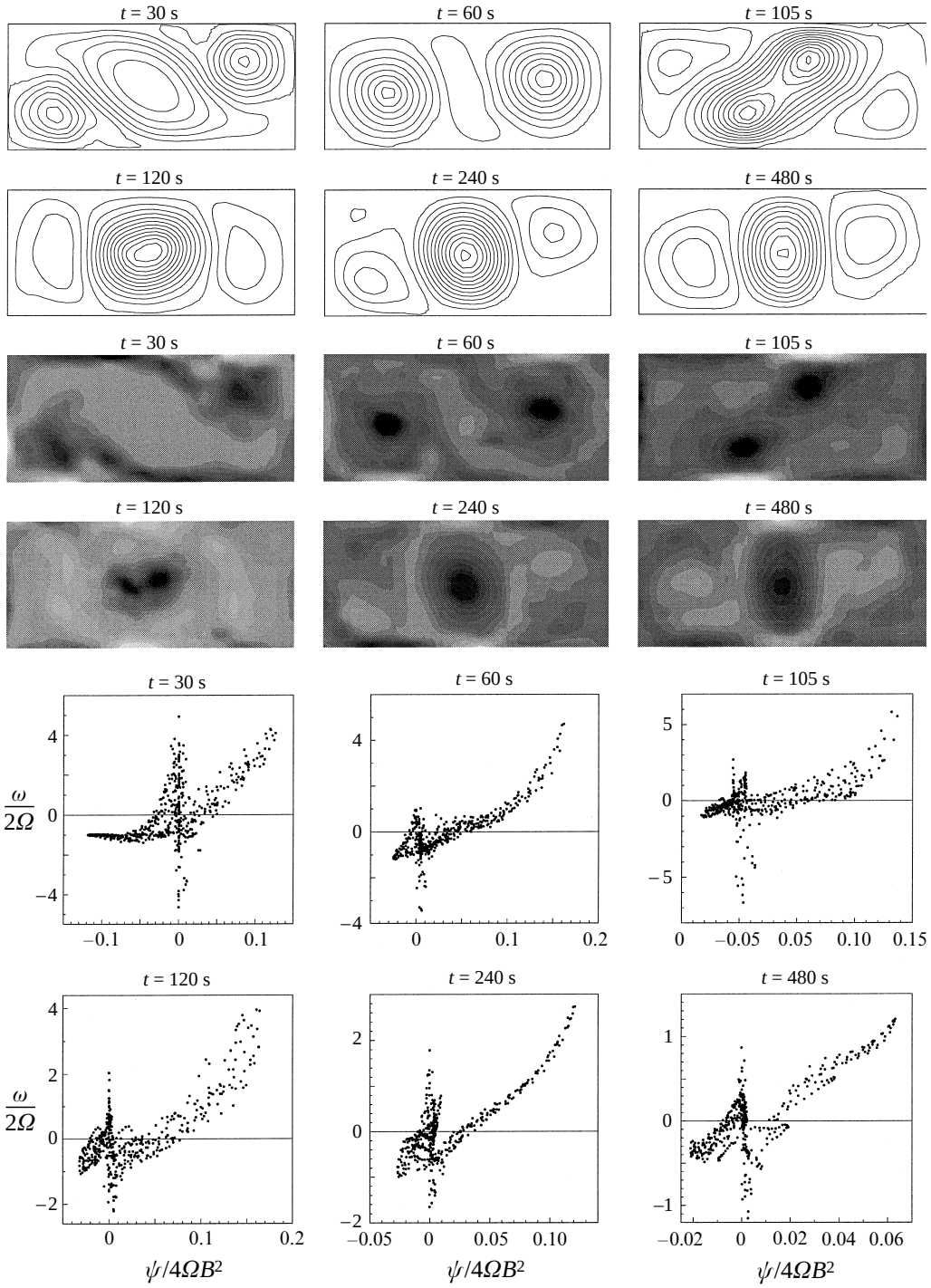

FIGURE 7. Experimental results for spin-up from 0 → 0.24 rad s^{-1} in a rectangular tank with length 0.886 m, width 0.389 m and depth 0.35 m.

results obtained by Montgomery & Joyce (1974) and Robert & Sommeria (1991) for the relationship between ω and ψ of the most likely vortex structure in inviscid flows. Their methods are technically different, but both rely on the counting of allowable dynamical states. The final equilibrium state of an initial vorticity distribution is calculated by introducing and maximizing the entropy of the vorticity field. In the method by Montgomery & Joyce, point vortices are used to represent the vorticity field. A well-known result of this approach is that if the vorticity distribution consists of the same number of positive and negative point vortices with equal strength, the relation between ω and ψ becomes a hyperbolic sine:

$$\omega = \omega_0 \sinh(\beta\psi). \tag{5.1}$$

The method by Robert & Sommeria is more complex and departs from a regular vorticity distribution. If the initial flow field consists of thin shear layers in an otherwise irrotational environment, such that the distribution of positive and negative vorticity is symmetric, the hyperbolic sine result of Montgomery & Joyce is recovered.

The vorticity distribution in a spin-up experiment, evolving from singular positive values at the sidewalls, meets this condition to a certain extent. It is therefore interesting to note that the $\omega(\psi)$-relations of newly formed cyclonic vortices in many spin-up experiments in this paper are characterized by a sinh-like upward curvature, in particular if the Reynolds number is high; if the vortices are very small or if the angular velocity is very low, the relationship becomes approximately linear. The cause of this difference may be the better conservation of the singularity of the initial vorticity distribution if the Reynolds number is high, or the outer parts of the vortices being turbulent and therefore more homogenized.

5.3. *Spin-up from 0 to 1.0 rad s^{-1}*

Results of the $0 \rightarrow 1.0$ rad s^{-1} experiment are presented in figure 8. Initially, the experiment looks essentially the same as the $0 \rightarrow 0.24$ rad s^{-1} experiment discussed in §5.2. The corner vortices are formed in much the same way, and merging occurs at approximately the same dimensionless time Ωt. However, where in the $0 \rightarrow 0.24$ rad s^{-1} experiment the resulting cyclonic vortex remained in the central position, in this case it appears to drift towards one of the southwest corners. A simple explanation for this behaviour can be given in terms of the influence of the free surface in combination with the effect of the sidewalls. Assuming that the central vortex is slightly off-centred, it will tend to move to the northwest, that is, in a clockwise spiroid motion towards the centre of the tank. However, as the vortex moves in westward direction, it approaches one of the longer sidewalls, and is deflected away from the centre. Apparently, this effect overcomes the northward component of the topographically induced drift, so that the central position of the cyclonic vortex becomes unstable. The vorticity graphs at $t = 72$ s and 96 s show that the centre of the cyclonic vortex is indeed shifted to one of the longer sidewalls. The drift of cyclonic vortices to the southwest corner is typical of spin-up experiments with sufficiently high angular velocities. It will be shown in §5.4 that this effect may even prevent the occurrence of merging. The hypothesis that the southwest drift of cyclonic vortices is caused by free-surface curvature is confirmed by the following three observations.

(*a*) The effect becomes stronger if the final angular velocity is increased.

(*b*) The effect becomes stronger if the depth is decreased, which is difficult to explain if the free surface does not play any role.

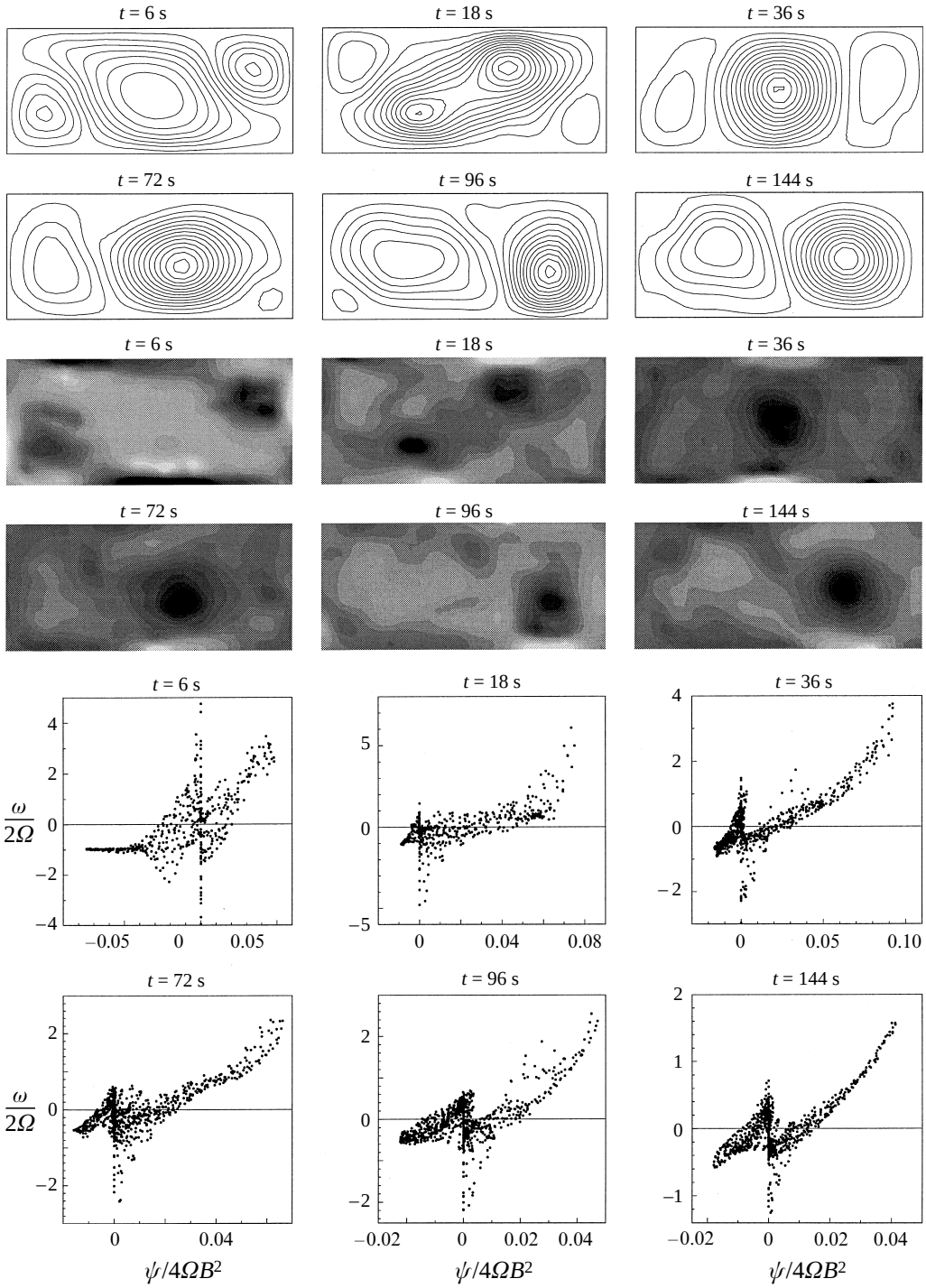

FIGURE 8. Experimental results for spin-up from $0 \rightarrow 1.0$ rad s^{-1} in a rectangular tank with length 0.886 m, width 0.389 m and depth 0.35 m.

(*c*) Experiments at a lower angular velocity but with bottom topography resembling the deformation of the free surface show a similar behaviour. Some of these experiments are discussed in §6.

The small amount of scatter in the $\omega(\psi)$-graph indicates that the flow is quasi-steady, but the flow pattern keeps changing in the course of the experiment, and although some states exist for many vortex turnover times, no definitive streamline pattern is observed in this experiment.

5.4. *Spin-up from 0 to 1.7 rad s*$^{-1}$

An angular velocity of 1.7 rad s^{-1} is the highest value that could be obtained with the available experimental equipment. At this rotation speed the difference in water height between the centre and the corners is several centimetres, or about 10% of the total depth. In about 20% of the experiments performed at this angular velocity, merging of the cyclonic corner vortices no longer occurs. If the fluid depth is decreased, this percentage increases to 100%, reflecting a stronger impact of the relative changes in depth due to a deformation of the surface. Thus, one may expect that for spin-up in the geometry discussed in this subsection, a value of 1.7 rad s^{-1} is somewhat below a critical value beyond which the occurrence of merging becomes unlikely. Neither the critical value for the transition from non-merging to merging at 0.1 rad s^{-1} nor the critical value for the transition from merging to non-merging due to free-surface effects is very well-defined. In the former case it may be unclear whether or not merging occurs because the process is incomplete and the cyclonic vortices do not really wrap around each other; in the latter case the difference between the occurrence and non-occurrence of merging is much more distinct, but turbulence introduces a certain randomness in the flow, suggesting a statistical interpretation of the critical value.

In figure 9, results are shown of one of the experiments in which merging does not occur; this is the more unlikely outcome of the experiment, but more illustrative than the more regular evolution, which is similar to the results of the $0 \rightarrow 1.0$ rad s^{-1} experiment (figure 8). The cyclonic corner vortices are formed very rapidly, and the central anticyclonic region is reduced to a weak, deformed structure. Instead of moving towards each other, the cyclones now move to the southwest corners, the anticyclonic cell being re-established in the process. The cyclonic vortices are affected by both the topography of the free surface and the presence of the sidewalls, and move in more or less circular trajectories (see figure 10) through the deeper parts of the tank. Then, after 50 turnover times, they suddenly and simultaneously move in a matter of seconds to the centre, and still merge into a single vortex. In this particular experiment, the flow loses some of its symmetry during this merging; in the $\omega(\psi)$-graph at $t = 120$ s in figure 9, one can see a secondary branch corresponding to a small vortex in the right-hand side of the tank that has no counterpart in the left-hand side. However, after a long time the flow regains most of its symmetry, and remains quasi-steady thereafter. In this regime one can observe a gradual evolution of the branch shape in the $\omega(\psi)$-graph due to Ekman suction. Additional experiments have been performed to check whether the retarded inward motion of the cyclonic vortices is reproducible. Most of these experiments were performed with smaller depths in order to avoid early merging. In all these experiments a similar behaviour was observed.

It is not entirely clear why the cyclonic vortices still move to the centre after spending such a long time in the deeper parts. The streamline and vorticity graphs at $t = 88$ s might give the impression that the motion of the cyclonic vortices is

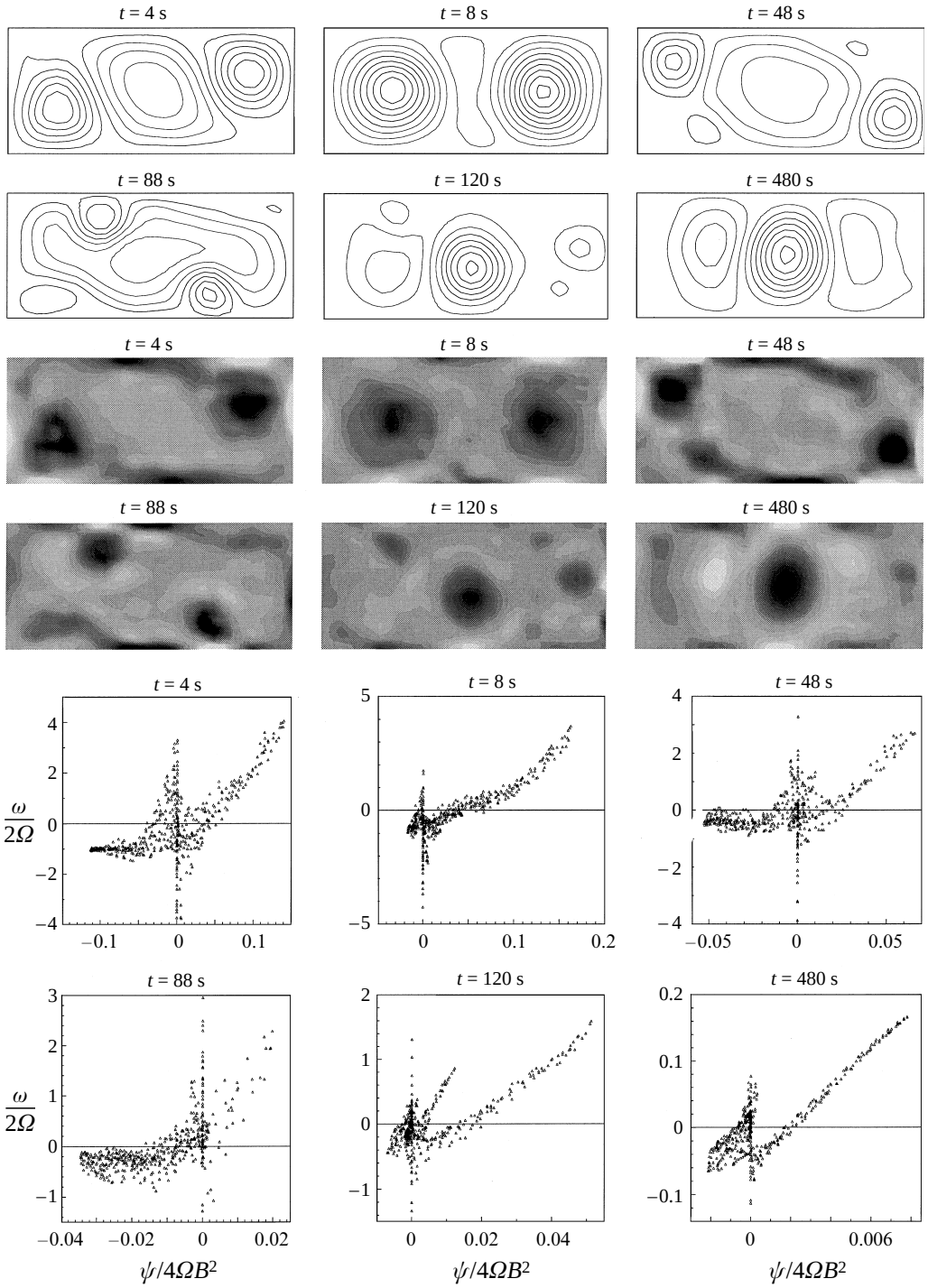

FIGURE 9. Experimental results for spin-up from $0 \rightarrow 1.7$ rad s^{-1} in a rectangular tank with length 0.886 m, width 0.389 m and depth 0.35 m.

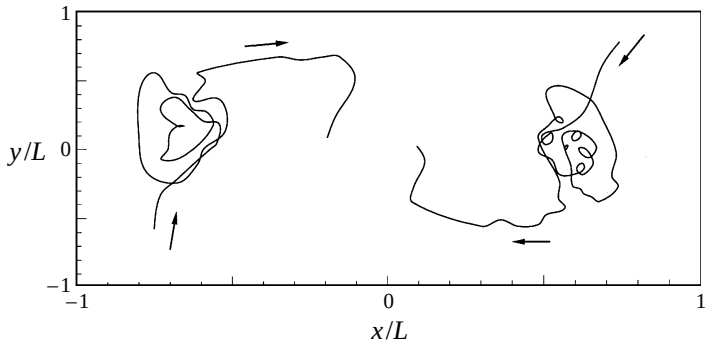

FIGURE 10. Trajectories of the centres of the cyclonic vortices from their formation at $t = 0$ to the merging at $t = 90$ s.

			
$0 \rightarrow 0.035$ rad s^{-1}	–	–	–
$0 \rightarrow 0.24$ rad s^{-1}	+	–	+
$0 \rightarrow 1.0$ rad s^{-1}	+	–	+
$0 \rightarrow 1.7$ rad s^{-1}	+/–	–	+

FIGURE 11. Occurrence of merging of the corner vortices in a tank of 88.6 × 38.9 cm filled to a depth of 35 cm. The symbols + and − indicate that merging does or does not occur, respectively.

driven by their image vortices, but this effect tends to drive the vortices back into the corners. One can think of a number of causes for this retarded merging. From $t = 8$ to 88 s, the strength of the cyclonic vortices, measured by the extremal value of the stream function, has decayed by a factor 8, whereas the extremal value of the stream function of the central anticyclonic vortex has increased by a factor 2. Thus, the regions with cyclonic vorticity become increasingly more passive, until they are taken along with the more persistent anticyclonic flow, which at $t = 88$ s fills nearly the entire domain.

Another cause might be that the motion rule for vortices over topography does not apply under all circumstances. Obviously the drift will depend on the degree of nonlinearity, the vorticity distribution of the vortex under consideration and the shape of the topography. So far it has been assumed that the free surface is always parabolic, which at the beginning of the experiment is a very crude assumption. Owing to the decay of vortex motion, the deviation from a parabolic surface gradually becomes smaller, which will have consequences for the vortex drift. However, it seems unlikely that this effect alone is strong enough to cause the sudden and simultaneous motion of the cyclonic vortices toward the centre.

6. Influence of free-surface deformation

In order to investigate the role of topography for the drift of cyclonic vortices, two types of additional experiments were performed in the 88.6 × 38.9 cm tank.

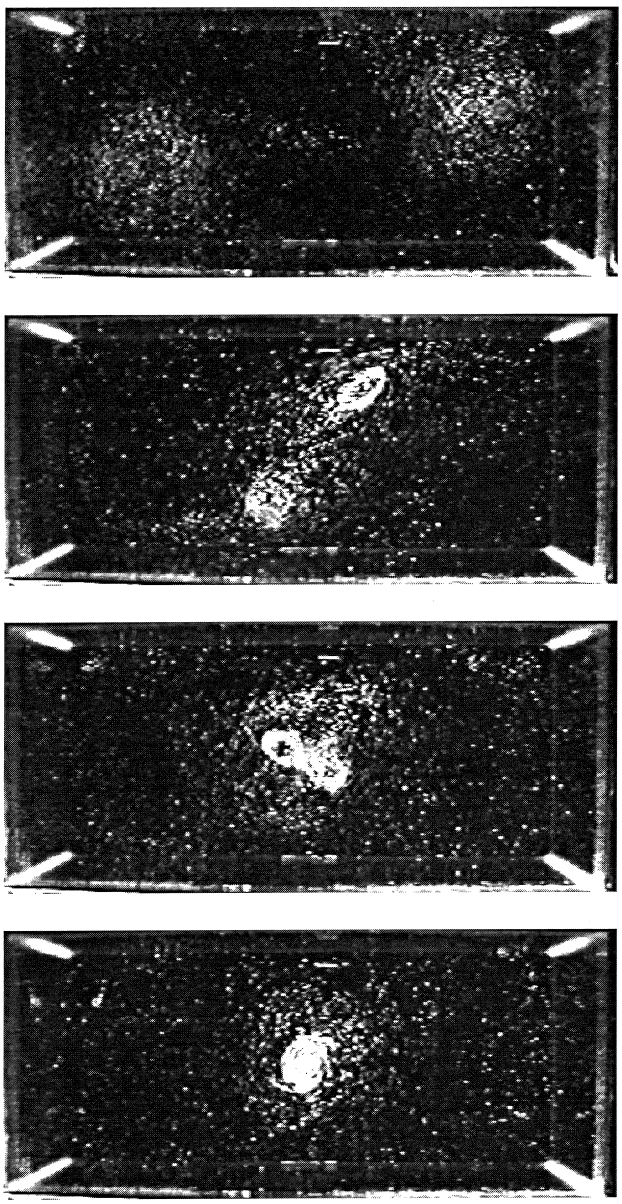

FIGURE 12. Merging of the corner vortices in a tank of 88.6 × 38.9 cm with a depth of 35 cm, covered with a rigid lid. The white dots correspond to paper particles at the bottom of the tank. The images were taken at 8, 14, 18 and 21 s, (*a*)–(*d*) respectively.

First, we used bottom topographies resembling the deformation of the free surface. These topographies consist of a false bottom made of two rigid plates as represented graphically in figure 11. In all experiments, the depth in the absence of the topography is 35 cm. The topography has a maximum elevation of 5 cm, which is of the same order as the deformation of the free surface at an angular velocity of 1.7 rad s^{-1}. The experiments with the sloping topography confirm the conjecture about the influence of the free surface. The topography with the highest point at the centre is similar to the deformation of the free surface, and so is the outcome of the evolution: at all

angular velocities, merging is prevented, and the flow field shows the same irregularity observed in experiments with high angular velocities and a flat bottom. The second topography is the reverse of the deformation of the free surface. In this case merging appears to be encouraged; the cyclonic vortices now drift to the centre of the tank, being the deepest part in this experiment.

Second, we repeated the $0 \rightarrow 1.7$ rad s^{-1} experiment in a tank with a rigid lid. In this way, deformation of the free surface is eliminated altogether. However, the presence of a rigid lid gives rise to a second Ekman layer. The influence of the Ekman layer at the rigid lid on the secondary flow can be eliminated by doubling the fluid depth, but unfortunately we did not have a tank at our disposal that was deep enough to realize this. Instead, we used a depth of 35 cm, the same as in the previous experiments. As the spin-up time scale $H/(2(\nu\Omega)^{1/2}) = 134$ s of the $0 \rightarrow 1.7$ rad s^{-1} experiment with rigid lid is still large compared with the time at which merging takes place, a comparison with the earlier experiments is still useful. As floating particles could not be used in this case, we seeded the fluid with small paper particles that were slightly heavier than water. These particles tend to accumulate at the centre of cyclonic vortices, and thus indicate whether or not merging occurs. The experiment was carried out 20 times, and in all cases merging occurred. The results of one of these experiments are shown in figure 12. The images lack the quality required for particle tracking, but show clearly the motion of the cyclonic vortices. At 8 s, two cyclonic vortices have been formed at two opposite corners of the tank. These vortices move towards the centre, and rapidly wrap around each other, resulting in a single cyclonic vortex. Thus, the experiments with a rigid lid confirm the conjecture that the non-occurrence of merging in the case of a free surface fluid at high angular velocities is caused by the curvature of the free surface.

7. Summary

The impulsive-spin-up flow in a rectangular tank can be divided into several stages. The relative flow field at the beginning of the experiment is characterized by a uniform vorticity -2Ω. The corresponding stream function as found by analytical means is in excellent agreement with experimental observations.

After this initial stage, the flow separates from the sidewall, and generally becomes organized into a small number of counter-rotating cells. The experiments confirm the conclusion drawn by van Heijst *et al.* (1990) that the flow tends to evolve towards a pattern consisting of an odd number of circular vortices that occupy the flow domain optimally.

The evolution of the flow field depends in the first place on the Reynolds number $\Omega L^2/\nu$. This becomes clear from the results of §§5.1 and 5.2, concerning the spin-up from rest to 0.035 rad s^{-1} resp. 0.24 rad s^{-1} in the same rectangular geometry. In both cases, strong cyclonic vortices are formed in two corners of the tank within one revolution time, but only in the experiment from 0 to 0.24 rad s^{-1} do these vortices appear to merge into a single vortex.

However, the curvature of the free surface may affect the formation of this cellular pattern, even if the elevation of the free surface is small compared with the depth of the fluid. The curved surface acts as a topographic plane, which is known from earlier research to induce a drift in individual vortices. This may be a determining factor for critical events such as merging of the cyclonic corner vortices early in the experiment, or may even cause a break-up of the pattern of aligned vortices that may be quasi-steady if the angular velocity is lower. The vortex drift also depends

on the presence of image vortices beyond the sidewalls. In particular, this may lead to a motion of cyclonic vortices to the deeper part of the tank, in contrast with their behaviour in an infinite domain. Thus, free-surface deformation is a discouraging factor for merging of the cyclonic vortices that are formed in the corners of the tank at the beginning of the experiment.

One of the authors (J. vd K.) gratefully acknowledges financial support from the Dutch Foundation of Fundamental Research (FOM).

REFERENCES

Boubnov, B. M. & Golitsyn, G. S. 1986 Experimental study of convective structures in rotating fluids. *J. Fluid Mech.* **167**, 503–531.

Boubnov, B. M. & Heijst, G. J. F. van 1994 Experiments on convection from a horizontal plate with and without background rotation. *Exps. Fluids* **16**, 155–164.

Carnevale, G. F., Kloosterziel, R. C. & Heijst, G. J. F. van 1991 Propagation of barotropic vortices over topography in a rotating tank. *J. Fluid Mech.* **233**, 119–139.

Dalziel, S. 1992 *DigImage. Image Processing for Fluid Dynamics.* Cambridge Environmental Research Consultants Ltd.

Greenspan, H. P. & Howard, L. N. 1963 On a time-dependent motion in a rotating fluid. *J. Fluid Mech.* **17**, 385–404.

Heijst, G. J. F. van 1989 Spin-up phenomena in non-axisymmetric containers. *J. Fluid Mech.* **206**, 171–191.

Heijst, G. J. F. van, Davies, P. A. & Davis, R. G. 1990 Spin-up in a rectangular container. *Phys. Fluids* A **2**, 150–159.

Heijst, G. J. F. van & Kloosterziel, R. C. 1989 Tripolar vortices in a rotating fluid. *Nature* **338**, 569–571.

Heijst, G. J. F. van, Kloosterziel, R. C. & Williams, C. W. M. 1991 Laboratory experiments on the tripolar vortex in a rotating fluid. *J. Fluid Mech.* **225**, 301–331.

Konijnenberg, J. A. van de, Andersson, H. I., Billdal, J. T. & Heijst, G. J. F. van 1994 Spin-up in a rectangular tank with low angular velocity. *Phys. Fluids* **6**, 1168–1176.

Konijnenberg, J. A. van de & Heijst, G. J. F. van 1995 Nonlinear spin-up in a circular cylinder. *Phys. Fluids* **7**, 2989–2999.

McWilliams, J. C. & Flierl, G. R. 1979 On the evolution of isolated, nonlinear vortices. *J. Phys. Oceanogr.* **9**, 1155–1182.

Montgomery, D. & Joyce, G. 1974 Statistical mechanics of negative temperature states. *Phys. Fluids* **17**, 1139–1145.

Nguyen Duc, J. M. & Sommeria, J. 1988 Experimental characterization of steady two-dimensional vortex couples. *J. Fluid Mech.* **192**, 175–192.

Plas, G.A.J. van der 1994 Introduction manual for particle tracking with DigImage. *Internal Rep.* R-1323-D. Faculty of Technical Physics, Fluid Dynamics Laboratory, Eindhoven University of Technology, The Netherlands.

Robert, R. & Sommeria, J. 1991 Statistical equilibrium states for two-dimensional flows. *J. Fluid Mech.* **229**, 291–310.

Rogers, M. H. & Lance, G. N. 1960 The rotationally symmetric flow of a viscous fluid in the presence of an infinite rotating disk. *J. Fluid Mech.* **7**, 617–631.

Stokes, G. G. 1843 On some cases of fluid motion. *Trans. Camb. Phil. Soc.*, vol viii. Reprinted in *Mathematical and Physical Papers*, vol I, Cambridge University Press (1880).

Suh, Y. K. 1994 Numerical study on two-dimensional spin-up in a rectangle. *Phys. Fluids* **6**, 2333–2344.

Wedemeyer, E. H. 1964 The unsteady flow within a spinning cylinder. *J. Fluid Mech.* **20**, 383–399.

Weidman, P. D. 1976 On the spin-up and spin-down of a rotating fluid. *J. Fluid Mech.* **77**, 685–708.